Print ISSN 2710-0200 *Full text available online at* *Ethiop J Nat Comp Sci.*
Electronic ISSN 2710-0219 *http://journal.uog.edu.et/index.php/EJNCS* *Vol. 3 (1) 431-442*
https://doi.org/*10.20372/ejncs/Ma.2022.14*

ORIGINAL RESEARCH

Dynamical Analysis of Cholera Diseases Transmission Model with Hospitalization

Haileyesus Tessema[1*] Gossay Aliy[1] Litegebe Wondie[1] Samuel Abebe[1] Sisay Ayanaw[1] Yehualashet Mengistu[1] Daniel Makinde[2] Hailay Weldegiorgis[3]

[1]Department of Mathematics, College of Natural and Computational Sciences, University of Gondar, Gondar, Ethiopia
[2]Faculty of Military Science, Stellenbosch University, Stellenbosch, South Africa
[3]Department of Mathematics, Mekelle University, Mekelle, Ethiopia

*Corresponding Author: haila.tessema@gmail.com

Received: 03 December 2022 / Accepted: 13 February 2023 / Published online: 19 February 2023
© The Author(s) 2023

Abstract

In this paper we developed a deterministic mathematical model of cholera disease dynamics by considering direct and indirect contact transmission pathway. The model considers five compartments, namely susceptible humans, infectious humans, hospitalized humans, recovered humans and the Vibrio cholera pathogen in the environment. The model qualitative behaviors, such as the invariant region, the existence of a positive invariant solution, the two equilibrium points (disease-free and endemic equilibrium), and their stabilities (local as well as global stability) of the model are studied. Moreover, the basic reproduction number of the model is obtained. Finally, we performed sensitivity analysis and numerical simulations. The numerical simulation results show that reducing contact rate, improving hospitalization rate, and environmental sanitation are the most important activities to fight against cholera disease from the community.

Keywords: Cholera, Vibro cholerae, DFE & EE, Stability Analysis, Numerical Simulation.

Introduction

Infectious diseases are still the leading cause of death and morbidity in the world. From this infectious diseases Cholera is a highly infectious disease which is endemic in many parts of Africa and Asia. It remains a significant public health threat in many countries worldwide mainly resource constrained settings (Usmani et al., 2021). Cholera infectious illness caused by infection of the intestine with the bacterium referred to as Vibrio cholera (Abubakar and Ibrahim, 2022). The disease is extremely virulent and kills very fast that remains a significant threat to public health in the developing world, with cyclic outbreaks occurring twice per year in endemic areas (Koelle, 2009). An estimated 3 -5 million cases and over 100,000 deaths occur each year around the world. The current ongoing cholera outbreak has occurred largely on the African continent, particularly sub-Saharan regions (Sun et al., 2017). More than 14 African countries (including Nigeria, Cameroon, Democratic Republic of Congo, South Sudan, Somalia, Ethiopia, Kenya, Tanzania, Zambia, Malawi, Mozambique, Zimbabwe, South Africa, Eswatini and Burundi) have reported cholera cases since the beginning of 2023.

2023).

Cholera is transmitted primarily by ingestion of contaminated water containing the bacterium Vibrio cholera and has plagued the world for centuries. The cholera bacterium is usually found in water or food sources that have been contaminated by feaces from a person infected with cholera (Usmani et al., 2021). Cholera is most likely to be found and spread in places with inadequate water treatment, poor sanitation, and inadequate hygiene (Gashaw Adane Erkyihun and Woldegiorgis, 2023). One can get cholera by drinking water or eating food contaminated with the cholera bacterium. It can be transmitted either by direct and indirect transmission pathways (Wang, 2022). Human-to-human (direct) way of cholera transmission is from the infected individual to the other individuals (touching, biting, and sexual intercourse). Whereas indirect (environment-to-human) way of transmission of cholera is through ingesting vibrio cholera bacteria from contaminated foods and waters. The disease can spread rapidly in areas with inadequate treatment of sewage and drinking water (Gashaw Adane Erkyihun and Woldegiorgis, 2023; Challa et al., 2022).

Epidemiologists and other researchers use mathematical modeling and numerical simulation for scientific understanding about the dynamics and preventive method of an infectious disease, for determining sensitivities, changes of parameter values, and forecasting. They use the most recent information to extrapolate the state and progress of an outbreak and make predictions. Several mathematical models on cholera were developed by different authors. From these research findings,some of the scholars used deterministic model (Nyabadza et al., 2019; Mukandavire and Morris Jr, 2015; Buliva et al., 2023; Yang et al., 2019; Sulayman, 2014) and some of the researchers used stochastic model (Tilahun et al., 2020; Iddrisu et al., 2023). Nyabadza et al. (2019), dynamics of cholera in the presence of limited resources. They showed that their model exhibits backward bifurcation and multiple equilibrium point they also concluded that the cases of cholera infection decrease if there are a sufficient number of hospital beds. A mathematical model for the transmission of cholera dynamics with a class of quarantined and vaccination parameter as control strategies is proposed by Ezeagu et al. (2019). They reached to a conclusion that effective quarantine, vaccination and proper sanitation reduce the disease contact rates that eliminates the spread of cholera. Onitilo et al. (2023) (2023),considered an SIR-V type of infection model for cholera dynamics. The other scholars used fractional order modeling (Rosa and Torres, 2021; Baba et al., 2023).The remaining scholars used optimal control strategies Berhe (2020); Bakare and Hoskova-Mayerova (2021); Abubakar and Ibrahim (2022).

But none of them consider the combined effect of cholera disease transmission(direct & indirect) with hospitalization of infectious individuals. In this paper we consider above gaps in the development of a cholera transmission dynamics mathematical model.

The organization of the study are: Section 1 is all about the background and literature review done studies. In section 2 the full description and formulation of the model is stated. In section 3 the model is analyzed. Section 4 is devoted on numerical simulation and calibration of the model. Our conclusions are discussed in section 5.

2 Model Description and Formulation

We divided the population denoted by N(t) according to the infection status into S(t)- susceptible, I(t)- infected, R(t)- recovered, and H(t)- hospitalized individuals at given time t. Moreover, C(t) is the amount of concentration of *Vibro cholerae* in an environment at time t. New susceptible individuals are recruited into the community at a rate of Π a birth or immigration rate of individuals, μ is the sum of the natural death rate and population-dependent death rate, or move to an infectious cohort by acquiring cholera through contact with the aquatic reservoir at a rate of $b\beta$.

Population in the susceptible compartment will be increased with a recruitment rate of Π. However, its number decreases by the natural causing death rate of μ and also moving to the infected compartment with the rate of $\lambda = b\beta C + \beta I$. Population in the infected compartment will be increased by the contact rate of λ, and also its number decreases by the natural causing death rate of μ, cholera causing death rate τ,and moving to the hospitalized compartment with the treatment rate of $(1-\alpha)\omega$ and the remaining $\alpha\omega$ proportion joins the recovered subpopulation. Population in the hospitalized compartment increases from the infected compartment with the treatment rate of $(1-\alpha)\omega$ and decreases with treatment with the recovery rate of φ and the natural causing death rate of μ. Population in the recovered compartment also increases by the recovery from treatment rate of φ and natural recovery $\alpha\omega$, but its number will decrease by the natural causing death

rate of μ. Infected individuals in the community shed the pathogen population of Vibrio cholera into the aquatic environment at rate of σ and at the rate of ϑ Vibrio cholera pathogen population dies and leave the community. Table 1 shows the description of model parameters. The flow diagram of the model is shown in Figure 1 below.

With regards to the above assumptions, the model is governed by the following system of differential equation:

$$\begin{aligned}
\frac{dS}{dt} &= \Pi - (b\beta\, C + \beta\, I)\, S - \mu\, S \\
\frac{dI}{dt} &= (b\beta\, C + \beta\, I)\, S - (\omega + \tau + \mu)\, I \\
\frac{dH}{dt} &= (1-\alpha)\,\omega I - (\mu + \varphi)\, H \\
\frac{dR}{dt} &= \alpha\,\omega I + \varphi H - \mu\, R \\
\frac{dC}{dt} &= \sigma\, I - \vartheta C
\end{aligned} \tag{1}$$

With the initial condition

$$S(0) = S_0 > 0\ , I(0) = I_0 \geq 0\ H(0) = H_0 \geq 0\ ,$$
$$R(0) = R_0 \geq 0\ , C(0) = C_0 \geq 0$$

3 Model Analysis

3.1 Invariant Region

Let us determine a region in which the solution of model (1) is bounded. For this model the total population is $N(S, I, H, R) = S(t) + I(t) + H(t) + R(t)$ and $C(t)$. Then, differentiating N with respect to time we obtain:

$$\frac{dN}{dt} = \frac{dS}{dt} + \frac{dI}{dt} + \frac{dH}{dt} + \frac{dR}{dt} = \Pi - \tau I - \mu N$$

If there is no death due to the disease, we get

$$\frac{dN}{dt} \leq \Pi - \mu N \tag{2}$$

After solving Equation (2) and evaluating it as $t \longrightarrow \infty$, we got $N(t) \longrightarrow \frac{\Pi}{\mu}$. Similarly,

$$\frac{dC}{dt} = \sigma\, I - \vartheta C \leq \sigma\, \frac{\Pi}{\mu} - \vartheta C \tag{3}$$

After solving Equation(3) and evaluating it as $t \longrightarrow \infty$, we got $C(t) \longrightarrow \frac{\sigma\Pi}{\vartheta\mu}$. Therefore, the feasible solution set of the system in equation (1) is the region given by:

$$\Omega = \Big\{ (S, I, H, R, C) \in \mathcal{R}_+^5 : 0 \leq S + I + H + R \leq \frac{\Pi}{\mu} C \leq \frac{\sigma\Pi}{\vartheta\mu} \Big\}$$

Which is the feasible solution set for the model (1) and all the solution set of (1) is bounded in it.

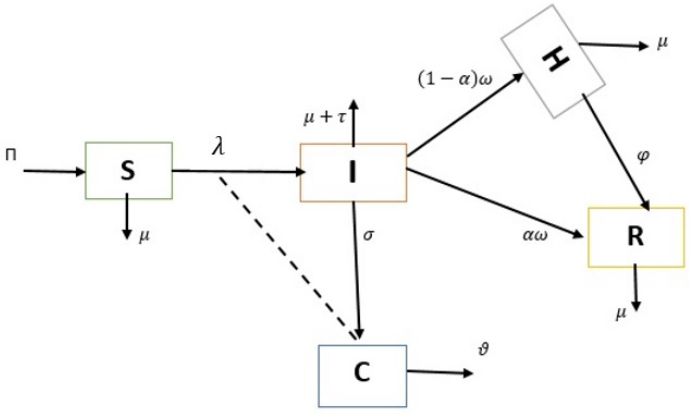

Figure 1: Flow chart of the pandemic Cholera disease transmission

3.2 Positivity of Solutions

Theorem 3.1. *If $S(0) > 0, I(0) > 0, H(0) > 0, R(0) > 0, C(0) > 0$ are positive in the feasible set Ω, then the solution set $(S(t), I(t), H(t), R(t), C(t))$ of system (1) is positive for all $t \geq 0$.*

Proof. : We let $\tau = sup\{t > 0 : S_0(\nu) \geq 0\ , I_0(\nu) \geq 0\ , H_0(\nu) \geq 0, R_0(\nu) \geq 0, C_0(\nu) \geq 0$ for all $\nu \in [0, t]\}$. Since $S_0(t) > 0\ , I_0(t) \geq 0\ , H_0(t) \geq 0\ R_0(t) \geq 0$ and $C_0(t) \geq 0$, hence $\tau > 0$. If $\tau < \infty$, then automatically $S_0(t)$ or $I_0(t)$ or $H_0(t)$ or $R_0(t)$or $C_0(t)$ is equal to zero at τ. Taking the first equation of the model

$$\frac{dS}{dt} = \Pi - (b\beta\, C + \beta\, I)\, S - \mu\, S \tag{4}$$

Then, using the variation of constants formula the solution of equation (4) at τ is given by

$$\begin{aligned}
S(\tau) = S_0 \exp\Big[- \int_0^\tau (b\beta\, C + \beta\, I + \mu)\, (S) ds \Big] \\
+ \int_0^\tau \Pi . \exp\Big[- \int_s^\tau (b\beta\, C \\
+ \beta\, I + \mu(\nu) d\nu ds > 0
\end{aligned}$$

Moreover, since all the variables are positive in $[0, \tau]$, $S(\tau) > 0$. It can be shown in a similar way that $I(\tau) > 0, H(\tau) > 0, R(\tau) > 0$, $C(\tau) > 0$. which is a contradiction. Hence $\tau = \infty$. Therefore, all the solution sets are positive for $t \geq 0$. Thus the model is meaningful and well-posed. Therefore, it is sufficient to study the dynamics of the model in Ω. □

3.3 Effective reproduction number & Cholera Free Equilibrium Point (DFE)

When there is no disease in the population, I.e $I = C = 0$, the disease free equilibrium occur and is obtained by taking the right side of Equation (1) equal to zero. Therefore the disease free equilibrium point is given by:

$$E_0 = (\frac{\Pi}{\mu}, 0, 0, 0, 0) \tag{5}$$

We calculate the Effective reproduction number $\mathcal{R}_0$ of the system by applying the next generation matrix method as laid out by (Van den Driessche and Watmough, 2002). The first step to get $\mathcal{R}_0$ is rewritten the model equations starting with newly infective classes:

$$\begin{array}{rcl} \frac{dI}{dt} & = & (b\beta\, C + \beta\, I)\, S - (\omega + \tau + \mu)\, I \\ \frac{dC}{dt} & = & \sigma I - \vartheta C \end{array} \tag{6}$$

Then by the principle of next-generation matrix, we obtained, The Jacobian matrices at DFE is given by

$$\mathcal{F} = \begin{pmatrix} \frac{\beta\,\Pi}{\mu} & \frac{b\beta\,\Pi}{\mu} \\ 0 & 0 \end{pmatrix}$$

and

$$\mathcal{V} = \begin{pmatrix} \omega + \tau + \mu & 0 \\ -\sigma & \vartheta \end{pmatrix}$$

$$\mathcal{F}\mathcal{V}^{-1} = \begin{pmatrix} \frac{\beta\,\Pi}{\mu\,(\omega+\tau+\mu)} + \frac{\Pi\, b\beta\,\sigma}{\mu\,(\omega+\tau+\mu)\vartheta} & \frac{b\beta\,\Pi}{\mu\,\vartheta} \\ 0 & 0 \end{pmatrix}$$

Therefore, the Effective reproduction number is given us

$$\begin{aligned} \mathcal{R}_{Eff} &= \frac{\beta\,\Pi\,(b\sigma + \vartheta)}{\mu\vartheta\,(\omega + \tau + \mu)} \\ &= \mathcal{R}^C_{Eff} + \mathcal{R}^I_{Eff} \end{aligned}$$

Tables 1: Description of parameters of the model (1).

Parameter	Description
Π	Recruitment rate of individuals
β	Contact rate of susceptible individuals
τ	Disease induced death rate of infected individuals
ϑ	Clearance rate of the bacteria.
φ	Treatment rate of hospitalized individuals .
ω	Proportion of exposed individuals leaving the compartment.
σ	Shading rate of infected individuals of the environment
μ	Natural death rate
α	Proportion of infected individuals to recovered .

where $\mathcal{R}^I_{Eff} = \frac{\beta\,\Pi\vartheta}{\mu\vartheta\,(\omega+\tau+\mu)}$ & $\mathcal{R}^C_{Eff} = \frac{\beta\,\Pi b\sigma}{\mu\,(\omega+\tau+\mu)}$

$\mathcal{R}_{Eff}$ is a threshold parameter that represents the average number of infection caused by one infectious individual when introduced in the susceptible population (Van den Driessche and Watmough, 2002).

Theorem 3.2. *The DFE point is locally asymptotically stable if $\mathcal{R}_{Eff} < 1$ and unstable if $\mathcal{R}_{Eff} > 1$.*

Proof. The Jacobian matrix, evaluated at the disease-free equilibrium E_0 is:

$$J = \begin{pmatrix} -\mu & -\frac{\beta\,\Pi}{\mu} & 0 & 0 & -\frac{b\beta\,\Pi}{\mu} \\ 0 & \frac{\beta\,\Pi}{\mu} - (\omega + \tau + \mu) & 0 & 0 & \frac{b\beta\,\Pi}{\mu} \\ 0 & (1-\alpha)\,\omega & -\mu - \varphi & 0 & 0 \\ 0 & \alpha\,\omega & \varphi & -\mu & 0 \\ 0 & \sigma & 0 & 0 & -\vartheta \end{pmatrix}$$

From the Jacobian matrix we obtained some of the eigenvalues are $-\mu, -(\mu + \eta)$ and the other eigenvalues are obtained from characteristic polynomial as

$$\lambda^2 + \psi_1\lambda + \psi_2 \tag{7}$$

Where $\psi_1 = \mu(\omega + \tau + \mu)\left[\frac{\vartheta}{\omega+\tau+\mu} + 1 - \mathcal{R}_{Eff}\right]$ and $\psi_2 = \mu\vartheta(\omega + \tau + \mu)(1 - \mathcal{R}_{Eff})$

We applied Routh-Hurwitz criteria and by the principle Equation (7) has strictly negative real root iff $\psi_1 > 0$, $\psi_2 > 0$ and $\psi_1\psi_2 > 0$. We see that both ψ_1 and ψ_2 are positive whenever $\mathcal{R}_{Eff} < 1$.

Hence the DFE is locally asymptotically stable if $\mathcal{R}_{Eff} < 1$. □

Theorem 3.3. *The equilibrium point E_0 of the model (1) is globally asymptotically stable if $\mathcal{R}_{Eff} < 1$ otherwise unstable.*

Proof. Consider the following Lyapunov function

$$L = \psi_1 I + \psi_2 C \tag{8}$$

Differentiating equation (8) with respect to t gives

$$\frac{dL}{dt} = \psi_1\frac{dI}{dt} + \psi_2\frac{dC}{dt} \tag{9}$$

Substituting $\frac{dI}{dt}$ and $\frac{dC}{dt}$ from the model (1), we get:

$$\begin{aligned} \frac{dL}{dt} &= \vartheta\left[\psi_1\frac{b\beta\Pi}{\vartheta\mu} - \psi_2\right] C \\ &+ \left[(\sigma + \tau + \mu)\left(\psi_1\frac{\beta\Pi}{\vartheta\mu\,(\sigma + \tau + \mu)} - 1\right) + \psi_2\sigma\right] I \end{aligned}$$

Here take $\psi_1 = \frac{\sigma}{\omega+\tau+\mu}\psi_2$, then we have

$$\begin{aligned} \frac{dL}{dt} &= \vartheta\psi_2\left[\frac{b\beta\Pi\sigma}{\vartheta\mu\,(\omega + \tau + \mu)} - 1\right] C \\ &+ \psi_2\sigma\left[\left(\frac{\beta\Pi}{\mu\,(\omega + \tau + \mu)} - 1\right) + 1\right] I \end{aligned}$$

Taking $\psi_2 = 1$, & substituting $\mathcal{R}_{Eff}$ we get

$$\frac{dL}{dt} = \vartheta\left(\mathcal{R}^C_{Eff} - 1\right)C + \sigma\mathcal{R}^I_{Eff} I$$

for $S \leq S^0 = \frac{\pi}{\mu}$ & $\frac{dV}{dt} \leq 0$ for $\mathcal{R}_{Eff} < 1$ and $\frac{dV}{dt} = 0$ if and only if $I = C = 0$. Thus, the system (1) on which $\frac{dV}{dt} \leq 0$ is E^0. Therefore by Lasalle's invariance principle, E_0 is globally asymptotically stable in Ω. □

3.4 The Endemic Equilibrium Point(EE)

The presence of disease in the population,$(S(t) > 0; I(t) \geq 0; H(t) \geq 0, R(t) \geq 0, C(t) \geq 0)$, there exist an equilibrium point called endemic equilibrium point denoted by $E^* = (S^*, I^*, H^*, R^*, , C^*) \neq 0$. It can be obtained by equating each equation of the model equal to zero. I.e

$$\frac{dS}{dt} = \frac{dI}{dt} = \frac{dH}{dt} = \frac{dR}{dt} = \frac{dC}{dt} = 0$$

Then we obtain

$$\begin{aligned}
S^* &= \frac{\vartheta\ (\omega + \tau + \mu)}{\beta\ (b\sigma + \vartheta)} \\
I^* &= \frac{\vartheta\mu\,(\mathcal{R}_{Eff} - 1)}{\beta\ (b\sigma + \vartheta)} \\
H^* &= \frac{(\alpha - 1)\mu\,\vartheta(\mathcal{R}_{Eff} - 1)}{(\mu + \varphi)\,(b\sigma + \vartheta)} \\
R^* &= \frac{(\alpha\mu + \varphi)\mu\,\vartheta(\mathcal{R}_{Eff} - 1)}{(\mu + \varphi)\,(b\sigma + \vartheta)} \\
C^* &= \frac{\sigma\mu\,(\mathcal{R}_{Eff} - 1)}{\beta\ (b\sigma + \vartheta)}
\end{aligned}$$

Theorem 3.4. *The endemic equilibrium E^* of system (1) is locally asymptotically stable in Ω if $\mathcal{R}_{Eff} > 1$.*

Proof. The Jacobian matrix of system (1) is given as

$$J = \begin{pmatrix}
-b\beta\,C - \beta\,I - \mu & -\beta\,S & 0 & 0 & -b\beta\,S \\
b\beta\,C + \beta\,I & \beta\,S - \mu - \omega - \tau & 0 & 0 & b\beta\,S \\
0 & (1-\alpha)\,\omega & -\mu - \varphi & 0 & 0 \\
0 & \alpha\,\omega & \varphi & -\mu & 0 \\
0 & \sigma & 0 & 0 & -\vartheta
\end{pmatrix} \tag{10}$$

From the Equation (10), we see that

$$\lambda - \mu = 0 \Rightarrow \lambda_1 = -\mu < 0 \quad and$$

$$\lambda - (\mu + \varphi) = 0 \Rightarrow \lambda_2 = -(\mu + \varphi) < 0$$

The remaining eigenvalues are obtained from evaluating from characteristic polynomial as

$$\lambda^3 + \varphi_1\lambda^2 + \varphi_2\lambda + \varphi_3 = 0 \tag{11}$$

Where

$$\begin{aligned}
\varphi_1 = \left[\frac{\sigma\mu(\omega + \tau + \mu)}{\vartheta(b\sigma + \vartheta)}\right](\beta(b\sigma + \vartheta) - 1) \\
+\beta(\vartheta + \mu) + \mu(\mathcal{R}_0 - 1) > 0, \quad if \quad \beta(b\sigma + \vartheta) > 1 \\
\varphi_2 = \chi_1 - \chi_2 > 0, \quad if \quad \chi_1 > \chi_2 \\
\varphi_3 = \mu\vartheta(\omega + \tau + \mu)\mathcal{R}_{Eff} > 0
\end{aligned}$$

where

$$\begin{aligned}
\chi_1 = ((\omega + \tau)(\sigma + \vartheta) + \vartheta(\vartheta + \mu))\left[\frac{\mu(\mathcal{R}_{Eff} - 1)}{b\sigma + \vartheta}\right] \\
+\mu(\omega + \tau + \mu)(\vartheta + \mu)) + \vartheta\mu \\
\chi_2 = \left[\frac{b\sigma\mu(\vartheta + \mu)(\mathcal{R}_{Eff} - 1)}{b\sigma + \vartheta}\right] + \frac{\sigma\mu(\omega + \tau + \mu)}{b\sigma + \vartheta} \\
+\vartheta(\omega + \tau + \mu)
\end{aligned}$$

Using Routh-Hurwitz criterion we have got that all roots of characteristic polynomial equation have negative real parts if and only if $\varphi_1 > 0, \varphi_2 > 0, \varphi_3 > 0$ and $\varphi_1\varphi_2 - \varphi_3 > 0$ for $\mathcal{R}_{Eff} > 1$. Hence, the endemic equilibrium E^* is locally asymptotically stable. □

3.5 Bifurcation analysis

A bifurcation is a qualitative change in the nature of the solution trajectories due to a parameter change. The point at which this change take place is called a bifurcation point. At the bifurcation point, a number of equilibrium points, or their stability properties, or both, change. We investigate the nature of the bifurcation by using the method, which is based on the use of the center manifold theory, introduced in (Castillo-Chavez and Song, 2004).

Theorem 3.5. *(Castillo-Chavez and Song, 2004)) Let us consider a general system of ODE's with a parameter ϕ:*

$$\frac{dx}{dt} = f(x, \phi), f : R^n \times R \longrightarrow R^n, f \in C^2(R^n \times R) \tag{12}$$

Where $x = 0$ is an equilibrium point for the system in Equation (12). That is $f(0, \phi) \equiv 0$ for all ϕ. Assume the following

M$_1$ *: $A = D_x f(0,0) = (\frac{\partial f}{\partial x_j}(0,0))$ is the linearization matrix of the system given by (1) around the equilibrium 0 with ϕ evaluated at 0. Zero is a simple eigenvalue of A and other eigenvalues of A have negative real parts;*

M$_2$ *: Matrix A has a nonnegative right eigenvector w and a left eigenvector v corresponding to the zero eigenvalue. Let f_k be the k^{th} component of f and*

$$a = \sum_{k,i,j=1}^{n} v_k w_i w_j \frac{\partial^2 f_k}{\partial x_i \partial x_j}(0,0)$$

$$b = \sum_{k,i=1}^{n} v_k w_i \frac{\partial^2 f_k}{\partial x_i \partial \phi}(0,0)$$

The local dynamics of (1) around 0 are totally determined by a and b.

i . $a > 0, b > 0$. When $\phi < 0$ with $|\phi| \ll 1$, 0 is locally asymptotically stable and there exists a positive unstable equilibrium; when $0 < \phi \ll 1, 0$ is unstable and there exists a negative, locally asymptotically stable equilibrium;

ii . $a < 0, b < 0$. When $\phi < 0$ with $|\phi| \ll 1$, 0 is unstable; when $0 < \phi \ll 1, 0$is locally asymptotically stable equilibrium, and there exists a positive unstable equilibrium;

iii . $a > 0, b < 0$. When $\phi < 0$ with$|\phi| \ll 1, 0$ is unstable, and there exists a locally asymptotically stable negative equilibrium; when $0 < \phi \ll 1, 0$ is stable, and a positive unstable equilibrium appears;

iv . $a < 0, b > 0$. When ϕ changes from negative to positive, 0 changes its stability from stable to unstable. Correspondingly a negative unstable equilibrium becomes positive and locally asymptotically stable.

In particular, if $a < 0$ and $b > 0$,then the bifurcation is forward; if $a > 0$ and $b > 0$,then the bifurcation is backward. Using this approach, the following result may be obtained:

Theorem 3.6. *The model in system(1) exhibits forward bifurcation at $\mathcal{R}_{Eff} = 1$.*

Proof. : We prove using center manifold theorem (Castillo-Chavez and Song, 2004) the possibility of bifurcation at $\mathcal{R}_{Eff} = 1$. Let $S = x_1$, $I = x_2$, $H = x_3$, $R = x_4$ and $C = x_5$. In addition, using vector notation $x = (x_1, x_2, x_3, x_4)^T$, and $\frac{dx}{dt} = F(x)$, with $F = (f_1, f_2, f_3, f_4)^T$, then model in system (1) re-written in the form:

$$\begin{array}{rcl} \frac{dx_1}{dt} & = & \Pi - (b\beta\, x_5 + \beta\, x_2)\, x_1 - \mu\, x_1 \\ \frac{dx_2}{dt} & = & (b\beta\, x_5 + \beta\, x_2)\, x_1 - (\omega + \tau + \mu)\, x_2 \\ \frac{dx_3}{dt} & = & (1-\alpha)\, \omega x_2 - (\mu + \varphi)\, x_3 \\ \frac{dx_4}{dt} & = & \alpha\, \omega x_2 + \varphi x_3 - \mu\, x_4 \\ \frac{dx_5}{dt} & = & \sigma\, x_2 - \vartheta x_5 \end{array} \tag{13}$$

We consider the disease transmission rate β as a bifurcation parameters so that $\mathcal{R}_{Eff} = 1$ iff

$$\beta = \beta^* = \frac{\mu\vartheta\,(\omega + \tau + \mu)}{\Pi\,(b\sigma + \vartheta)}$$

The disease free equilibrium is given by $(x_1 = \frac{\Pi}{\mu}, x_2 = 0; x_3 = 0, x_4 = 0, x_5 = 0)$. Then the linearizion matrix of Equation (13) at a disease free Equilibrium is given by:

$$J = \begin{pmatrix} -\mu & -\frac{\beta\,\Pi}{\mu} & 0 & 0 & -\frac{b\beta\,\Pi}{\mu} \\ 0 & \frac{\beta\,\Pi}{\mu} - (\omega + \tau + \mu) & 0 & 0 & \frac{b\beta\,\Pi}{\mu} \\ 0 & (1-\alpha)\,\omega & -\mu - \varphi & 0 & 0 \\ 0 & \alpha\,\omega & \varphi & -\mu & 0 \\ 0 & \sigma & 0 & 0 & -\vartheta \end{pmatrix} \tag{14}$$

Zero is a simple eigenvalue of J if $\mu = 1$. The right eigenvector, $w = (w_1, w_2, w_3, w_4)^T$, associated with this simple zero eigenvalue can be obtained from $Jw = 0$. The system becomes

$$\begin{array}{rcl} -\mu w_1 - \frac{\beta^*\Pi}{\mu} w_2 - \frac{b\beta^*\Pi}{\mu} w_5 & = & 0 \\ \frac{\beta^*\Pi}{\mu} - (\omega + \tau + \mu) w_2 + \frac{\beta^*\Pi}{\mu} w_5 & = & 0 \\ (1-\alpha)\omega w_2 - (\varphi + \mu) w_3 & = & 0 \\ \alpha\omega w_2 + \varphi w_3 + \mu w_4 & = & 0 \\ \sigma w_2 - \vartheta w_5 & = & 0 \end{array} \tag{15}$$

From Equation(15) we obtain

$$w_1 = -\frac{(\omega + \tau + \mu)}{\mu\Pi})w_2, w_2 = w_2 > 0,$$

$$w_3 = \frac{(1-\alpha)\omega}{\varphi + \mu} w_2, w_4 = \frac{\omega(1-\alpha) + \omega(\varphi + \mu)}{\mu(\varphi + \mu)} w_2,$$

$$w_5 = \frac{\sigma}{\vartheta} w_2$$

Here we have taken into account the expression for β^* . Next we compute the left eigenvector, $v = (v_1, v_2, v_3, v_4)$, associated with this simple zero eigenvalue can be obtained from $vJ = 0$ and the system becomes

$$\begin{array}{c} -\mu v_1 = 0 \\ -\frac{\beta^*\Pi}{\mu} v_1 - (\frac{\beta^*\Pi}{\mu} + (\omega + \tau + \mu)) v_2 - (1-\alpha)\omega v_3 + \alpha\omega v_4 \\ +\sigma v_5 = 0 \\ -(\varphi + \mu) v_3 + \varphi v_4 = 0 \\ -\mu v_4 = 0 \\ -\frac{b\beta^*\Pi}{\mu} v_1 + (\frac{b\beta^*\Pi}{\mu} + (\omega + \tau + \mu)) v_2 - (1-\alpha)\omega v_3 + \alpha\omega v_4 \\ +\vartheta v_5 = 0 \end{array} \tag{16}$$

From Equation (16), we obtain

$$v_1 = v_3 = v_4 = 0, v_5 = \frac{b(\omega + \tau + \mu)}{b\sigma + \vartheta} v_2,$$

Here we have taken into account the expression for β^*. where v_2 is calculated to ensure that the eigenvectors satisfy the condition $v.w = 1$. Since the first, third and fourth component of v are zero, we don't need the derivatives of f_1, f_3 and f_4. From the derivatives of f_2 and f_5 the only ones that are nonzero are the following:

$$\frac{\partial^2 f_2}{\partial x_1 \partial x_5} = \frac{\partial^2 f_2}{\partial x_5 \partial x_1} = \beta^*,$$

$$\frac{\partial^2 f_2}{\partial x_2 \partial x_3} = \frac{\partial^2 f_2}{\partial x_3 \partial x_2} = b\beta^*$$

with

$$\frac{\partial^2 f_2}{\partial x_2 \partial \beta^*} = \beta^*, \frac{\partial^2 f_2}{\partial x_5 \partial \beta^*} = b\beta^*$$

and all the other partial derivatives of f_2 and f_4 are zero. The direction of the bifurcation at $\mathcal{R}_0 = 1$ is determined by the signs of the bifurcation coefficients a and b, obtained from the above partial derivatives,

given respectively by

$$a = -2\frac{\beta(\omega+\tau+\mu)}{\mu\Pi}\left[1+\frac{b\sigma}{\vartheta}\right] < 0 \tag{17}$$

and

$$b = \beta\left[1+\frac{b\sigma}{\vartheta}\right] > 0 \tag{18}$$

Since the coefficient b is always positive and the sign of the coefficient a is negative. Therefore, cholera model to exhibit a forward bifurcation and there exist at least one stable endemic equilibrium when $\mathcal{R}_{Eff} > 1$. Using expression for I^* in the endemic equilibrium, we plotted a forward bifurcation diagram in Figure 2. □

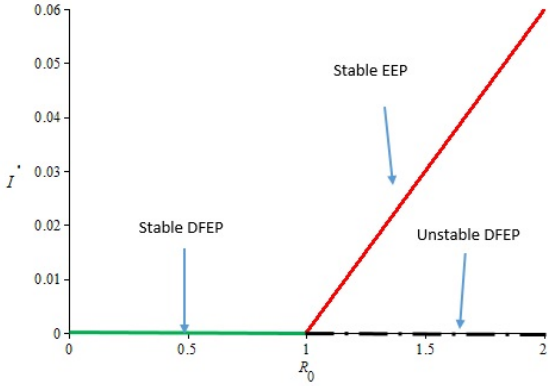

Figure 2: Forward bifurcation drawn by utilizing $I$the parameter values listed in Table 2

3.6 Sensitivity Analysis

In this section we have done sensitivity analysis to identify parameters that have an impact in the transmission of cholera. We used the normalized sensitivity index definition as defined in (Blower and Dowlatabadi, 1994) as it is done by (Alemneh et al., 2023). The Normalized forward sensitivity index of a variable, $\mathcal{R}_{Eff}$, that depends differentiable on a parameter, p, is defined as:

$$\Lambda_p^{\mathcal{R}_{Eff}} = \frac{\partial \mathcal{R}_{Eff}}{\partial p} \times \frac{p}{\mathcal{R}_{Eff}}$$

for p represents all the basic parameters. Here we have $\mathcal{R}_{Eff} = \frac{\beta\,\Pi\,(b\sigma+\vartheta)}{\mu\vartheta\,(\omega+\tau+\mu)}$. For the sensitivity index of $\mathcal{R}_{Eff}$ to the parameters:

$$\Lambda_\beta^{\mathcal{R}_{Eff}} = \frac{\partial \mathcal{R}_{Eff}}{\partial \beta} \times \frac{\beta}{\mathcal{R}_{Eff}} = 1 > 0$$
$$\Lambda_b^{\mathcal{R}_{Eff}} = \frac{\partial \mathcal{R}_{Eff}}{\partial b} \times \frac{b}{\mathcal{R}_{Eff}} = \frac{b\sigma}{b\sigma+\vartheta} > 0$$
$$\Lambda_\mu^{\mathcal{R}_{Eff}} = \frac{\partial \mathcal{R}_{Eff}}{\partial \alpha} \times \frac{\mu}{\mathcal{R}_{Eff}} = -\frac{\mu}{\omega+\tau+\mu} < 0$$
$$\Lambda_\tau^{\mathcal{R}_{Eff}} = \frac{\partial \mathcal{R}_{Eff}}{\partial \tau} \times \frac{\tau}{\mathcal{R}_{Eff}} = -\frac{\tau}{\omega+\tau+\mu} > 0$$
$$\Lambda_\omega^{\mathcal{R}_{Eff}} = \frac{\partial \mathcal{R}_{Eff}}{\partial \omega} \times \frac{\omega}{\mathcal{R}_{Eff}} = -\frac{\omega}{\omega+\tau+\mu} < 0$$
$$\Lambda_\sigma^{\mathcal{R}_{Eff}} = \frac{\partial \mathcal{R}_{Eff}}{\partial \mu} \times \frac{\mu}{\mathcal{R}_{Eff}} = \frac{b\sigma}{b\sigma+\vartheta} < 0$$
$$\Lambda_\vartheta^{\mathcal{R}_{Eff}} = \frac{\partial \mathcal{R}_{Eff}}{\partial \vartheta} \times \frac{\vartheta}{\mathcal{R}_{Eff}} = -\frac{b\sigma}{b\sigma+\vartheta} < 0$$

Figure 3 shows the reproduction number's sensitivity indices in relation to the basic parameters. From Figure 3 we can conclude that, those parameters that have positive indices $\Pi, \beta,\ \ and\ \ \sigma$ show that they have great impact on expanding cholera disease in the community if their values are increasing by keeping other parameters constant. However, those parameters in which their sensitivity indices are negative $\tau, \omega, \vartheta,\ \ and\ \ \mu$ have an effect of minimizing the burden of cholera disease in the community as their values increase. From this result, we advise the government stakeholders should act on decreasing those positive indices parameters such us working to reduce the rate of intake of Vibrio Cholerae

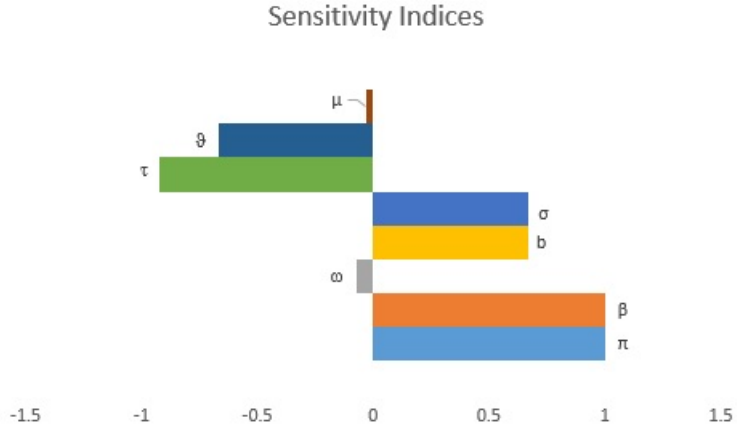

Figure 3: The local elasticity indices of $\mathcal{R}_{Eff}$ with respect to parameters of the model (1).

from infected humans(β) as well as decreasing shading rate of infected individuals Vibrio Cholerae in the environment decreases the reproduction number while increasing those parameters with negative indices such as increasing the rate of recovery (ω) of infected individuals from cholera and increasing a mechanism of clearance rate (ϑ) of Vibrio Cholerae decreases the reproduction to control cholera in the community.

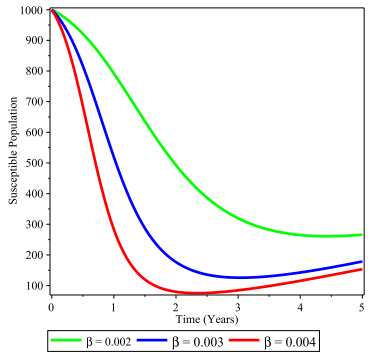

(a)

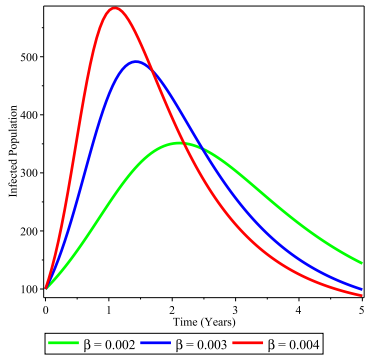

(b)

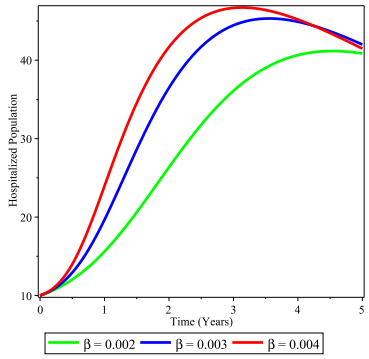

(c)

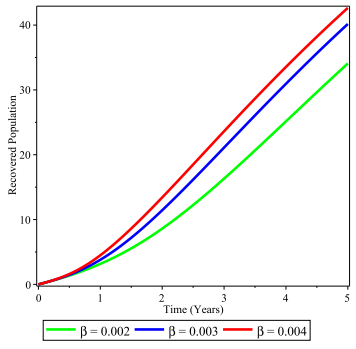

(d)

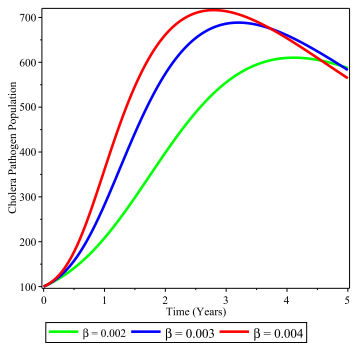

(e)

Figure 4: Simulations of the Cholera model for different value of β.

4 Numerical Simulations

We perform some numerical simulations of system (3) to support our theoretical findings.We employed Maple software for simulation of the model in equation (1) and done with ODE45. Using the parameter values from Table 2, and the initial conditions S(0) = 1000, I(0) = 100,R(0)=0 H(0) = 10, C(0) = 100. We

Tables 2: parameter values for Cholera model in 1

Parameter symbol	**Value**	**Source**
Π	3.5	Assumed
β	0.002	(Berhe, 2020)
b	2	Assumed
σ	20	Assumed
ω	0.062	Assumed
α	0.44	(Berhe, 2020)
μ	0.0014	(Alemneh et al., 2023)
ϑ	0.033	(Berhe, 2020)
τ	0.015	(Berhe, 2020)
φ	0.2	(Tilahun et al., 2020)

investigated numerically the effect of the parameters on the spread of Cholera in a population.

Fig. 4 (a)-(e), showed the effect of varying the contact rate of susceptible individuals with the *Vibro cholerae* pathogen in the environment β and infected individuals. As the value of β increases from 0.002 to 0.006 the susceptible population Fig. 4 (a) decreases in number and the other populations like,infected Fig. 4 (b), hospitalized Fig. 4 (c),recovered Fig. 4 (d) and *Vibro cholerae* pathogen Fig.4 (e) increases in their number as time runs. This is therefore, reducing means of contact with the *Vibro cholerae* and infectious individuals brings down the number of infected individuals in the population.

We have showed the effect of varying the number of individuals who leave the infected sub-population ω in the Fig. 5 (a)-(e). As the value of ω increases from 0.032 to 0.082 , increases the susceptible population in Fig. 5 (a), hospitalized in Fig. 5 (c) and recovered in Fig. 5 (d) and decreases the number of infected population Fig. 5 (b), *Vibro cholerae* pathogen in Fig. 5 (e). Hence it is advisable to increase the value of ω to fight against the disease.

In Fig. 6 (a)-(e), We have shown the sensitivity of shading rate of infectious individuals to cholera pathogen in the environment σ. As the value of σ increases from 0.2 to 0.5 the Cholera pathogen in the environment increases as shown in Fig. 6 (e). This pathogen increment again increases the number of infected population Fig. 6 (b), hospitalized Fig. 6 (c), recovered population Fig. 6 (d) and on the other side it decreases the number of susceptible population Fig. 6 (a) as time runs. Therefore, it is important to reduce the shading rate of infectious individuals to the environment to reduce the disease from the community.

5 Discussions and Conclusions

This study considered an SIHR-C deterministic model to analyze cholera disease. In this research we analyzed the qualitative behaviour of the basic model. From this analysis we obtained the effective reproduction number of the model. Using this number, we showed the stability of the disease free and endemic equilibrium point of the model.

We utilized lyapunov function to prove the global stability of DFE point. From the Bifurcation analysis our model exhibits forward bifurication which does not agree with the findings of Sun et al. (2017). This may be because of the model assumption that we used mass action incidence. A sensitivity analysis of the model is done to show the importance of model parameters. It can be inferred from sensitivity that positive indices β, σ, π should be decreased while increasing negative indices ω, τ, ϑ have a great impact on the transmission dynamics and prevalence of cholera this was recommended done by Berhe (2020).

Hence, we conclude that the rate of indirect and direct contact must be minimized to reduce the number of infected individuals as it is similar to the findings of work done by Tilahun et al. (2020).

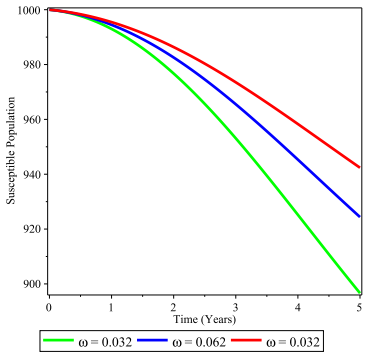

(a)

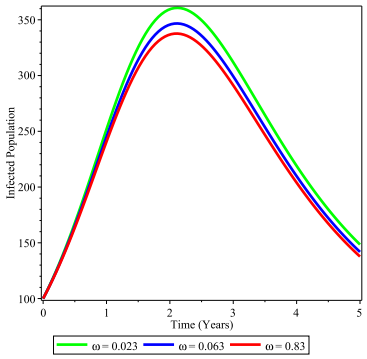

(b)

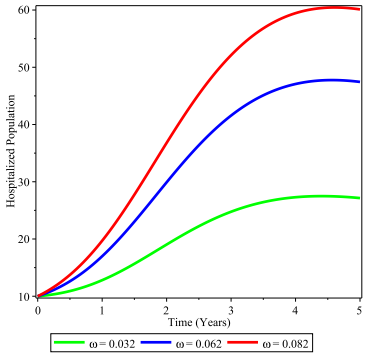

(c)

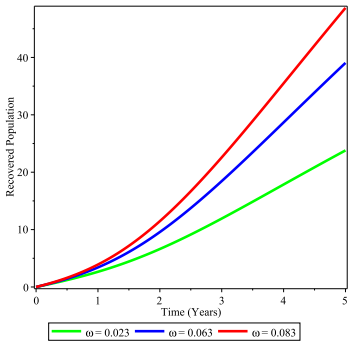

(d)

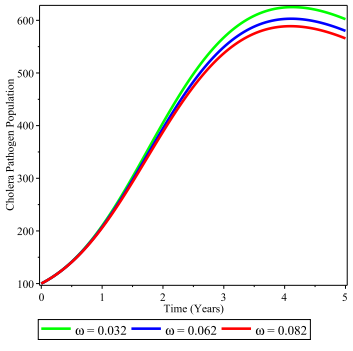

(e)

Figure 5: Simulations of the Cholera model for different value of ω.

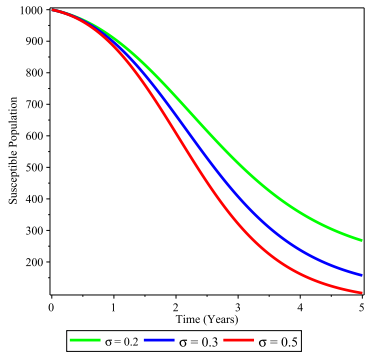

(a)

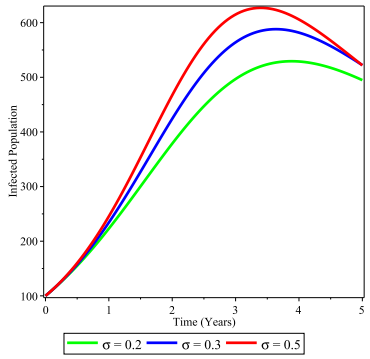

(b)

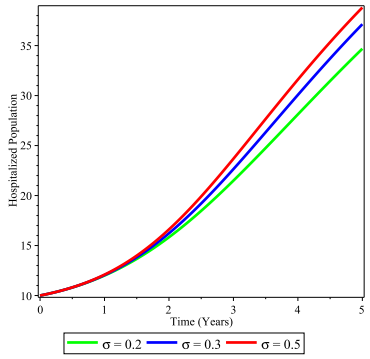

(c)

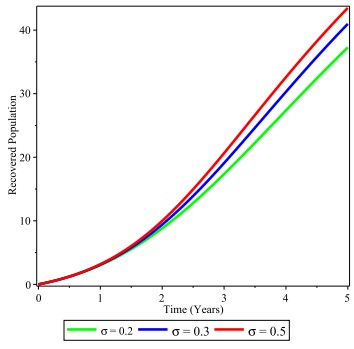

(d)

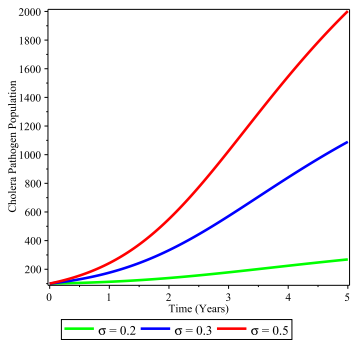

(e)

Figure 6: Simulations of the Cholera model for different value of σ.

Also, we found that working on enhancing the treatment of infected individuals reduces infections individual's this will decrease contribution in the parasite pathogen concentration in the environment Tilahun et al. (2020).

Therefore, decision makers and stakeholders can apply the results that have a significant contribution in combating this pandemic in very short period of time.

Data Availability

The data we used for this research is from respective published articles that are cited.

Conflict of Interest

The authors declare that there is no conflict of interest of their work.

Acknowledgments

We would like to express our heartfelt appreciation to the anonymous reviewers for their constructive comments.

References

Abubakar S. F., and Ibrahim M. (2022). Optimal control analysis of treatment strategies of the dynamics of cholera. *Journal of Optimization*, 2022.

Alemneh H. T., Belay A. M., et al. (2023). Modelling, analysis, and simulation of measles disease transmission dynamics. *Discrete Dynamics in Nature and Society*.

Baba I. A., Humphries U. W., and Rihan F. A. (2023). A well- posed fractional order cholera model with sat- urated incidence rate. *Entropy*, 25:360.

Bakare E. A. and Hoskova-Mayerova S. (2021). Optimal control analysis of cholera dynamics in the presence of asymptotic transmission. *Axioms*, 10:60.

Berhe H. W. (2020). Optimal control strategies and cost-effectiveness analysis applied to real data of cholera outbreak in ethiopia's oromia region. *Chaos, Solitons & Fractals*, 138:109933.

Blower S. M. and Dowlatabadi H. (1994). Sensitivity and uncertainty analysis of complex models of diseasetransmission: an hiv model, as an example. *International Statistical Review/Revue Internationale de Statistique*, pages 229–243.

Buliva E., Elnossery S., Okwarah P., Tayyab M., Brennan R., and Abubakar A. (2023). Cholera prevention, control strategies, challenges and world health organization initiatives in the eastern mediterraneanregion: A narrative review. *Heliyon*.

Castillo-Chavez C. and Song B. (2004). Dynamical models of tuberculosis and their applications. *Mathematical biosciences and engineering*, 1:361–404.

Challa J. M., Getachew T., Debella A., Merid M., Atnafe G., Eyeberu A., Birhanu A., and Regassa L. D. (2022). Inadequate hand washing, lack of clean drinking water and latrines as major determinants of cholera outbreak in somali region, Ethiopia in 2019. *Frontiers in public health*, 10:845057.

Ezeagu N. J., Togbenon H. A., and Moyo E. (2019). Modeling and analysis of cholera dynamics with vacci- nation. *American Journal of Applied Mathematics and Statistics*, 7:1–8.

Gashaw N. A., Erkyihun A., and Woldegiorgis A. Z. (2023). The threat of cholera in Africa. *Zoonoses*, 42:1–6.

Iddrisu W. A., Iddrisu I., Iddrisu A.-K. (2023). Modeling cholera epidemiology using stochastic

Koelle K. (2009). The impact of climate on the disease dynamics of cholera. Clinical Microbiology and Infection, 15:29–31.

Mukandavire Z. and Morris Jr J. G. (2015). Modeling the epidemiology of cholera to prevent disease transmission in developing countries. Microbiology spectrum, 3(3):10 –1128.

Nyabadza, F. Aduamah J. M., and J. Mushanyu. (2019). Modelling cholera transmission dynamics in the presence of limited resources. BMC Research Notes, 12:1–8.

Onitilo S., Usman M., Daniel D., Odule T., and Sanus, I A. (2023). Modelling the transmission dynamics of cholera disease with the impact of control strategies in Nigeria. Cankaya University Journal of Science and Engineering, 20:35–52.

Rosa S. and Torres D. F. (2021). Fractional-order modelling and optimal control of cholera transmission. Fractal and Fractional, 5:261.

Sulayman F. (2014). Modelling and analysis of the spread of cholera disease in Nigeria with environmental control. Research thesis.

Sun G.-Q., Xie J.-H., S.-H. Huang, Z. Jin, M.-T. Li, and Liu. L. (2017). Transmission dynamics of cholera: Mathematical modeling and control strategies. Communications in Nonlinear Science and Numerical Simulation, 45:235–244.

Tilahun G. T., Woldegerima W. A., and Wondifraw A. (2020). Stochastic and deterministic mathematical model of cholera disease dynamics with direct transmission. Advances in Difference Equations, 2020(1):1–23.

Usmani M., K. D. Brumfield, Y. Jamal, A. Huq, R. R. Colwell, and A. Jutla. A review of the environmental trigger and transmission components for prediction of cholera. Tropical Medicine and Infectious Disease, 6:147.

Van den Driessche P. and Watmough J. (2002). Reproduction numbers and sub-threshold endemic equilibria for compartmental models of disease transmission. Mathematical biosciences, 180:29–48.

Wang J. (2022). Mathematical models for cholera dynamics - a review. Microorganisms, 10:2358.

Yang J., Modnak C., and Wang J. (2019). Dynamical analysis and optimal control simulation for an agestructured cholera transmission model. *Journal of the Franklin Institute*, 356:8438–8467.